

Nanoclusters of Gold on a High-Area Support: Almost Uniform Nanoclusters Imaged by Scanning Transmission Electron Microscopy

Alper Uzun,[†] Volkan Ortalan,[†] Yalin Hao,[†] Nigel D. Browning,^{†,*} and Bruce C. Gates^{†,*}

[†]Department of Chemical Engineering and Materials Science, University of California, Davis, One Shields Avenue, Davis, California 95616 and [‡]Lawrence Livermore National Laboratory, Livermore, California 94550

Since the discovery of unprecedented catalytic properties of highly dispersed gold nanoparticles on oxide supports, extensive effort has gone into probing the effects of the nanoparticle size on the catalytic activity, especially for CO oxidation. The identities of the catalytically active species continue to be vigorously debated, with candidates including gold clusters with typical diameters of several nanometers and Au atoms at the gold-support interface;^{1,2} the most active catalysts may be those with gold clusters with diameters even less than several nanometers.^{1,3} In attempts to elucidate the nature of the gold species, theoretical methods have been used to compare the reactivities of various gold sites,^{4–10} and numerous experiments have been done with model catalysts consisting of gold dispersed on planar supports exemplified by TiO₂ single crystals.^{11–14}

These investigations are limited because (a) the theoretical reports (except for a few^{4–7}) have neglected the role of the support, which, however, is generally regarded as having a significant influence on the catalytic properties^{15,16} and (b) the planar supports have lacked surface hydroxyl groups, which may influence the gold chemistry, in particular the oxidation states of the Au atoms at the gold-support interface.¹⁷

Investigations of gold dispersed on typical catalyst supports, which are porous, high-area oxides, on the other hand, suffer from the intrinsic nonuniformity of the support surfaces and the lack of control of the sizes of the gold nanoparticles; in general, these samples consist of mixtures of gold nanoparticles varying in size from a few at-

ABSTRACT Highly dispersed supported gold offers unprecedented catalytic properties. Determination of the dependence of the catalytic properties on the gold nanocluster size requires the preparation of size-controlled gold nanoclusters on support surfaces with a high degree of uniformity. Starting from site-isolated mononuclear gold complexes on high-area MgO, we demonstrate the preparation of gold clusters consisting of <10 atoms. These samples have been imaged with atomic resolution by aberration-corrected scanning transmission electron microscopy. The images show that treatment of the supported mononuclear complexes at 318 K in flowing helium caused aggregation of the gold into clusters of 2–6 atoms, present with unconverted individual site-isolated mononuclear gold species and in the absence of any larger nanoparticles. Treatment of the sample at a higher temperature (373 K) in flowing helium resulted in the formation of gold clusters with diameters of 0.58 ± 0.15 nm (containing roughly 10 Au atoms), again in the absence of larger nanoparticles. Upon exposure of the supported nanoclusters to the electron beam, they underwent aggregation to gold clusters approximately 1 nm in average diameter, as shown in consecutive STEM images.

KEYWORDS: gold · nanoparticles · nanoclusters · aberration-corrected STEM

oms to thousands of atoms, as evidenced by images recorded with electron microscopy.^{18–21}

Recently, Herzing *et al.*¹⁹ presented aberration-corrected scanning transmission electron microscopy (STEM) images of gold on an FeO_x support; their images demonstrated that gold species were present in mixtures including individual Au atoms (0.13 ± 0.07 atomic % of the gold), nanoclusters with nuclearities ranging from 3–4 atoms (*ca.* 0.2–0.3 nm in diameter), and nanoparticles with nuclearities up to approximately 5000 atoms (*ca.* 7 nm in diameter); the nanoparticles with diameters exceeding about 2 or 3 nm constituted 98.8 ± 0.8 atomic % of the gold. The data of Herzing *et al.*¹⁹ led them to infer that the activity of their catalyst for CO oxidation can be attributed to bilayer gold clusters with diameters of approximately 0.5 nm and consisting of approximately 10 Au atoms each.

*Address correspondence to bcgates@ucdavis.edu.

Received for review July 16, 2009 and accepted October 18, 2009.

Published online October 28, 2009.
10.1021/nn9008142 CCC: \$40.75

© 2009 American Chemical Society

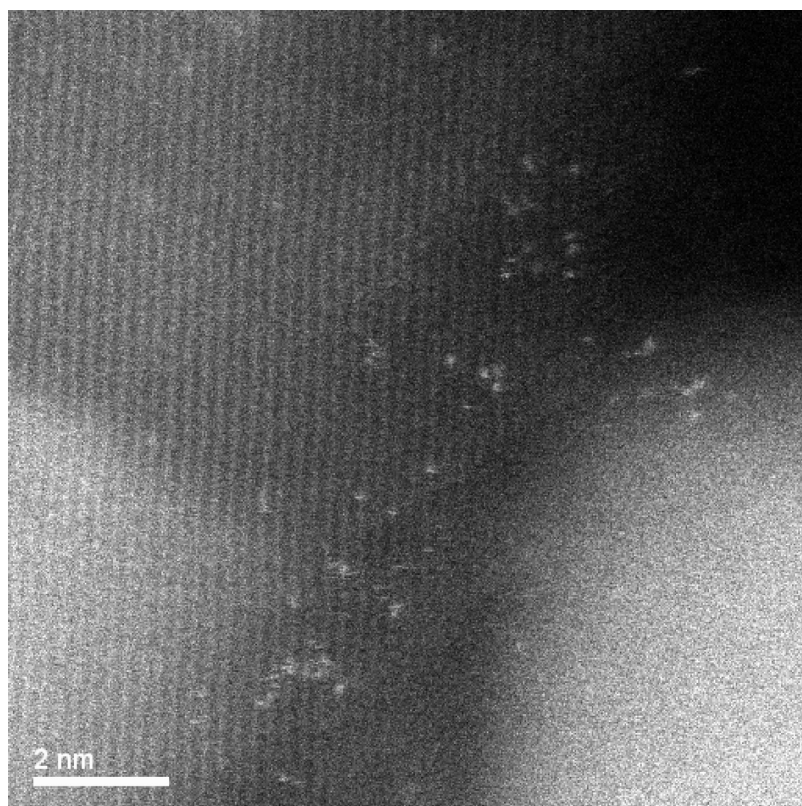


Figure 1. High-angle annular dark-field (Z-contrast) image of Sample B. The image shows gold nanoclusters consisting of only a few atoms each (less than 6) together with individual Au atoms in the absence of any larger gold clusters.

Rashkeev *et al.*²⁰ also presented STEM images of gold on TiO₂ characterized by a broad distribution of species ranging from single, isolated Au atoms to gold nanoparticles up to 5 nm in diameter.

Catalysts with such wide distributions of structures may be useful for the discovery of active or selective catalysts, because they include a wide range of potentially active and selective structures.²¹ However, the identification of which of the supported species are indeed the active or selective ones requires the preparation of size-controlled gold species on the supports—this preparation challenge is one of the major impediments to the elucidation of how supported gold catalysts work and which ones work best.²² Part of the difficulty of preparing supported gold clusters or particles with controlled sizes is that gold is easily (auto)reduced and aggregated into larger particles. There have been only a limited number of investigations demonstrating the preparation of supported clusters consisting of only a few Au atoms on high-area supports.

One approach was to synthesize gold clusters from a reactive precursor, Au(CH₃)₂(acac) [acac is CH₃COCHCOCH₃], with the clusters formed in the nanoscale cages of zeolites, which limited their size (but also limit their accessibility).²³ This precursor was also used with high-area MgO as a support,²⁴ and extended X-ray absorption fine structure (EXAFS) spectra of the samples prepared by treatment in helium at 373 K led

to the inference that the clusters could be approximated as Au₆, on average. Similarly, gold clusters consisting of approximately 10 Au atoms, on average, were prepared on high-area TiO₂ from the same precursor as the temperature was ramped to 390 K with the sample in flowing helium.²⁵ Furthermore, Bus *et al.*²⁶ treated a sample prepared by impregnation of γ -Al₂O₃ with HAuCl₄ in H₂ at 400 K to form gold clusters characterized by an average Au–Au coordination number of 3.8 determined by EXAFS spectroscopy, corresponding to clusters consisting of about 5 or 6 Au atoms each, on average.

In all of these examples, the supported gold was characterized spectroscopically, and direct evidence of the degree of uniformity of the gold species was missing; it was not known whether there were substantially larger nanoparticles of gold present with the nanoclusters consisting of only a few atoms each. Now we report images of samples prepared from Au(CH₃)₂(acac) on MgO. When the samples are treated under suitably mild conditions, the images show almost uniform gold nanoclusters, some containing only a few Au atoms—in the absence of sub-

stantially larger gold nanoparticles. The evidence was obtained by aberration-corrected STEM with atomic resolution to allow imaging of all the gold structures on the support.

EVIDENCE OF SUPPORTED GOLD NANOCLUSTERS

Imaging Supported Nanoclusters of Only a Few Au Atoms. The infrared (IR) and EXAFS data characterizing the sample (Sample A) prepared by the reaction of Au(CH₃)₂(acac) and calcined MgO demonstrate the presence of the mononuclear Au(CH₃)₂ complexes on the MgO surface, consistent with earlier results²⁷ (details are given in Supporting Information). Aberration-corrected STEM images confirm the presence of site-isolated mononuclear Au atoms in the absence of any detectable gold complexes, as reported elsewhere.²⁸

STEM images of the sample prepared by treatment of Sample A in flowing helium at 318 K (Sample B) show that the site-isolated mononuclear gold complexes initially present were no longer present alone on the surface; instead, some of the Au atoms had aggregated into clusters of only a few atoms each. Images show the presence of gold nanoclusters with 2–6 Au atoms along with some site-isolated Au atoms (Figure 1). These species were resolved only in regions of the samples where the focus was optimized.²⁹

These are the first images of such small gold nanoclusters in the absence of substantially larger gold clusters (those with more than about 6 Au atoms). We emphasize (a) that the reactive molecular precursor, $\text{Au}(\text{CH}_3)_2(\text{acac})$, was crucial to the preparation of these samples, *via* the site-isolated mononuclear gold complexes anchored to the MgO surface, and (b) that the preparation required mild conditions to minimize the degree of aggregation of the gold.

Moreover, the highly dehydroxylated MgO was a key to obtaining high-quality STEM images, because (a) the contrast between the light atoms of the support and the heavy Au atoms offers high contrast in the STEM images and (b) this support, after calcination at a high temperature (973 K), consists of essentially cubic microparticles that present flat, well-ordered surfaces that are well suited to imaging of the gold species on them with a single focus value.^{29,30} We recognize that the defect sites and the hydroxyl groups on MgO might play a role in stabilizing the gold in the form of clusters as small as the ones we report.

STEM images of the sample prepared by treating the Sample A in He at a higher temperature (373 K, Sample C) show, in contrast, formation of larger clusters than in Sample B (Figure 2a). The average cluster size was 0.58 ± 0.15 nm (with account taken of the blurring effects³¹), and even these clusters are markedly smaller than any other gold nanoclusters formed with a high degree of uniformity on a high-area support. The size distribution of the clusters is given in Figure 2b. Images obtained for a larger region of the sample with a lower magnification confirm the absence of any larger gold nanoparticles in this sample (Figure 3).

Gold nanoclusters with diameters less than about 1 nm, on average, supported on oxides, CeO_2 ³² and MgO ,³³ and prepared from $\text{Au}(\text{CH}_3)_2(\text{acac})$ according to a method similar to ours, have been found by EXAFS spectroscopy to be the average gold structures in working CO oxidation catalysts. EXAFS data characterizing the gold on MgO catalyst show that the activity for CO oxidation increased as the average gold cluster size increased in the range up to about 4–6 Au atoms per cluster, on average—just in the range we show here.³³ Because there are no images of these catalysts and therefore no evidence by which to determine the degree of uniformity of the gold species in them, the question remains about whether these cluster sizes are representative of the catalytically active species. The images presented here demonstrate how to make such small supported gold clusters with a high degree of uniformity.

Limited Stability of Sample in Electron Beam. We emphasize that we have restricted the results presented here to the first images that were obtained in each region. Subsequent images, in contrast, show effects of the electron beam, which caused Au atoms and clusters to migrate on the support and to form larger gold clusters.

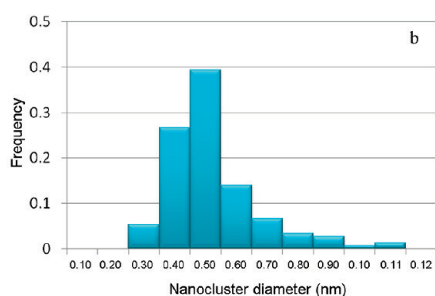
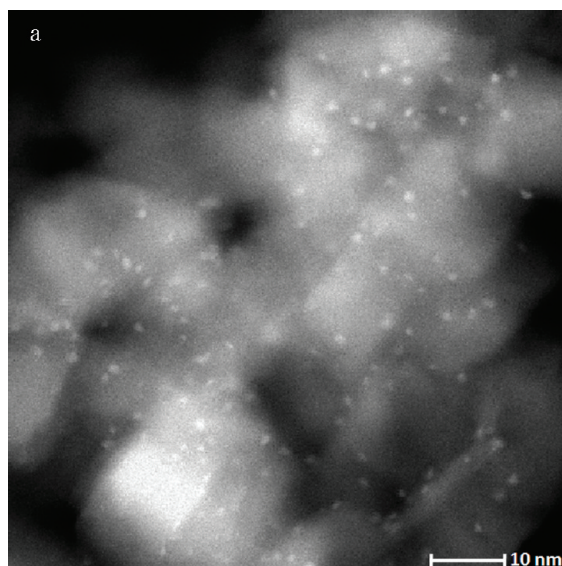


Figure 2. (a) High-angle annular dark-field (Z-contrast) image of Sample C. The image shows almost uniform subnanometer gold nanoclusters in bright contrast present in the absence of any larger gold clusters. (b) Histogram of the distribution of diameters of 150 gold nanoclusters in image a. The mean nanocluster diameter was 0.58 ± 0.15 nm.

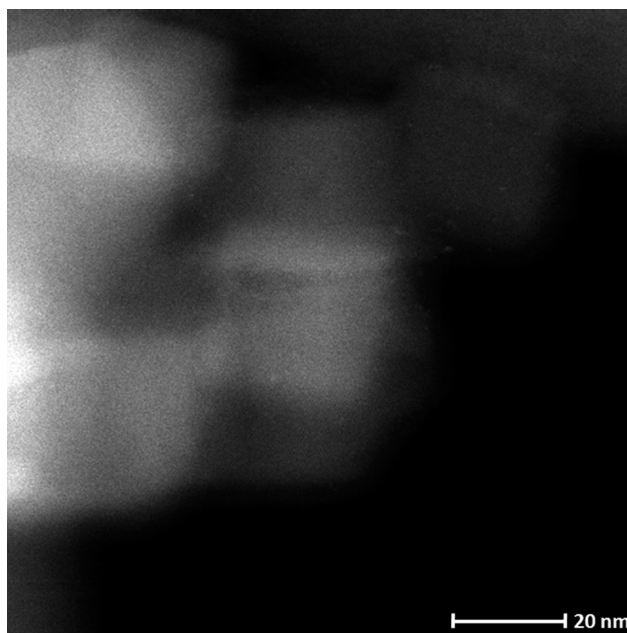


Figure 3. High-angle annular dark-field (Z-contrast) image of Sample C at a magnification lower than that of Figures 1 and 2. The image confirms the presence of subnanometer gold nanoclusters in the absence of any larger gold clusters.

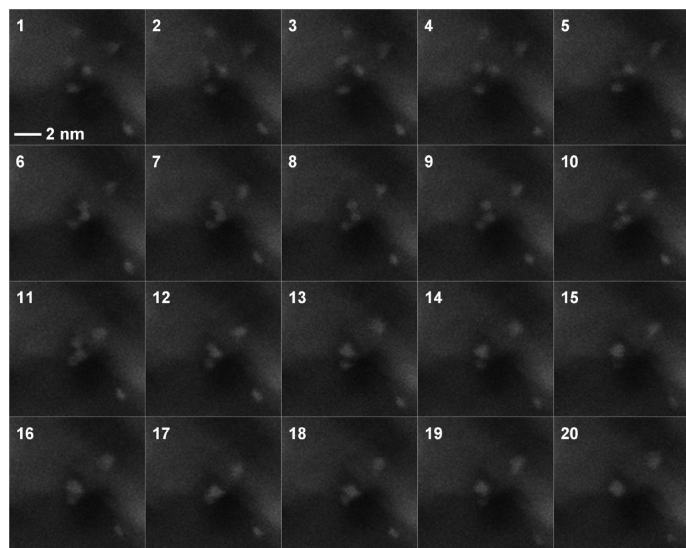


Figure 4. Consecutive STEM images characterizing a single region of Sample C. Each scan is denoted by the scan number as given in the upper left corner of each image. The changes in location, size, and brightness of the spots show the migration of gold nanoclusters to form a larger nanocluster under the influence of the electron beam.

Figure 4 (representing consecutive images taken of the same region with a time interval of approximately

20 s) shows how the electron beam caused the migration of gold nanoclusters with a diameter of 0.6 ± 0.1 nm (initially present in Sample C) to form a larger cluster, with a diameter of approximately 1 nm. Cluster migration and growth were evidenced by the formation of a brighter and a larger spot by the movement of initially present small bright spots in the consecutive images (images 1–20, Figure 4).

Others^{34–36} have reported evidence of comparable effects of the electron beam on supported metals.

CONCLUSIONS

A major challenge in the identification of the active species in supported gold catalysts is the preparation of gold nanoclusters with controlled sizes; the smaller the nanoclusters, the more challenging is the preparation. Here we show the conditions (318 K with the sample in helium) for preparation of size-controlled clusters of only a few Au atoms each on high-area MgO. The STEM images presented here are the first of such small nanoclusters in the absence of larger gold clusters on a high-area support. Treatment at higher temperatures and under the influence of the electron beam leads to migration and aggregation of the gold into large nanoparticles.

METHODS

Synthesis. The MgO powder was highly dehydroxylated by treatment in O₂ at 973 K (the resultant powder has a surface area of 100 m²/g). The initial supported gold sample (0.2 wt % Au) was prepared by the reaction of Au(CH₃)₂(acac) with MgO (EM Science) in an *n*-pentane slurry, as before.²⁶ The resultant sample (Sample A) was treated in flowing helium at atmospheric pressure as the temperature was ramped at 5 K/min to 318 K to give Sample B and, alternatively, to 373 K to give Sample C. Each sample was cooled quickly to room temperature once the target temperature had been reached in either preparation.

STEM Imaging. The images of the supported gold samples were obtained at Oak Ridge National Laboratory by high-angle annular dark field (HAADF) STEM with a FEI Titan microscope equipped with a high-brightness field emission gun and operated at 300 kV with a CEOS dodecapole probe aberration corrector. The samples were air sensitive and were therefore handled with extreme care to avoid exposure to the atmosphere; details of the sample handling are described in the Supporting Information.

Acknowledgment. This work was supported by DOE (A.U., Grant No. DE-FG02-04ER15600 and Y. H., Grant No. DE-FG02-04ER15513) and by the National Science Foundation (NSF) (V.O., Grant No. CTS-0500511). The STEM images were acquired at Oak Ridge National Laboratory's Shared Research Equipment User Facility, supported by the Division of Scientific User Facilities, Basic Energy Sciences, DOE.

Supporting Information Available: Sample handling for STEM imaging and additional STEM images. This material is available free of charge via the Internet at <http://pubs.acs.org>.

REFERENCES AND NOTES

- Haruta, M. Size- And Support-Dependency in the Catalysis of Gold. *Catal. Today* **1997**, *36*, 153–166.
- Bond, G. C.; Thompson, D. T. Gold-Catalysed Oxidation of Carbon Monoxide. *Gold Bull.* **2000**, *33*, 41–52.
- Hutchings, G. J. Heterogeneous Catalysts-Discovery and Design. *J. Mater. Chem.* **2009**, *19*, 1222–1235.
- Wang, J. G.; Hammer, B. Some Recent Theoretical Advances in the Understanding of the Catalytic Activity of Au. *Appl. Catal., A* **2005**, *291*, 21–31.
- Laursen, S.; Linic, S. Oxidation Catalysis by Oxide-Supported Au Nanostructures: The Role of Supports and the Effect of External Conditions. *Phys. Rev. Lett.* **2006**, *97*, 026101-1–026101-4.
- Sicolo, S.; Di Valentin, C.; Pacchioni, G. Formation of Cationic Gold Clusters on the MgO Surface from Au(CH₃)₂(acac) Organometallic Precursors: A Theoretical Analysis. *J. Phys. Chem. C* **2007**, *111*, 5154–5161.
- Remediakis, I. N.; Lopez, N.; Nørskov, J. K. CO Oxidation on Rutile-Supported Au Nanoparticles. *Angew. Chem., Int. Ed.* **2005**, *44*, 1824–1826.
- Prestianni, A.; Ciofini, A. M.; Labat, F.; Adamo, C. CO Oxidation on Cationic Gold Clusters: A Theoretical Study. *J. Phys. Chem. C* **2008**, *112*, 18061–18066.
- Coquet, R.; Howard, K. L.; Willock, D. J. Theory and Simulation in Heterogeneous Gold Catalysis. *Chem. Soc. Rev.* **2008**, *37*, 2046–2076.
- Huang, W.; Ji, M.; Dong, C.-D.; Gu, X.; Wang, L.-M.; Gong, X. G.; Wang, L.-S. Relativistic Effects and the Unique Low-Symmetry Structures of Gold Nanoclusters. *ACS Nano* **2008**, *2*, 897–904.
- Matthey, D.; Wang, J. G.; Wendt, S.; Matthiesen, J.; Schaub, R.; Lægsgaard, E.; Hammer, B.; Besenbacher, F. Enhanced Bonding of Gold Nanoparticles on Oxidized TiO₂(110). *Science* **2007**, *315*, 1692–1696.
- Tong, X.; Benz, L.; Metiu, H.; Bowers, M. T.; Buratto, S. K. Intact Size-Selected Au_n Clusters on a TiO₂(110)-(1 × 1) Surface at Room Temperature. *J. Am. Chem. Soc.* **2005**, *127*, 13516–13518.
- Lee, S.; Fan, C.; Wu, T.; Anderson, S. L. CO Oxidation on Au_n/TiO₂ Catalysts Produced by Size-Selected Cluster Deposition. *J. Am. Chem. Soc.* **2004**, *126*, 5682–5683.
- Lee, S.; Molina, L. M.; López, M. J.; Alonso, J. A.; Hammer, B.; Lee, B.; Seifert, S.; Winans, R. E.; Elam, J. W.; Pellin, M. J.

- Vajda, S. Selective Propene Epoxidation on Immobilized Au_{6–10} Clusters: The Effect of Hydrogen and Water on Activity and Selectivity. *Angew. Chem., Int. Ed.* **2009**, *48*, 1467–1471.
15. Comotti, M.; Li, W.-C.; Spliethoff, B.; Schüth, F. Support Effect in High Activity Gold Catalysts for CO Oxidation. *J. Am. Chem. Soc.* **2006**, *128*, 917–924.
16. Fierro-Gonzalez, J. C.; Gates, B. C. Catalysis by Gold Dispersed on Supports: The Importance of Cationic Gold. *Chem. Soc. Rev.* **2008**, *37*, 2127–2134.
17. Fierro-Gonzalez, J. C.; Guzman, J.; Gates, B. C. Role of Cationic Gold in Supported CO Oxidation Catalysts. *Top. Catal.* **2007**, *44*, 103–114.
18. Tompos, A.; Margitfalvi, J. L.; Szabó, E. G.; Pászti, Z.; Sajó, I.; Radnóczy, G. J. Role of Modifiers in Multicomponent MgO-Supported Au Catalysts Designed for Preferential CO Oxidation. *J. Catal.* **2009**, *266*, 207–217.
19. Herzing, A. A.; Kiely, C. J.; Carley, A. F.; Landon, P.; Hutchings, G. J. Identification of Active Gold Nanoclusters on Iron Oxide Supports for CO Oxidation. *Science* **2008**, *321*, 1331–1335.
20. Rashkeew, S. N.; Lupini, A. R.; Overbury, S. H.; Pennycook, S.; Pantelides, S. T. Role of the Nanoscale in Catalytic CO Oxidation by Supported Au and Pt Nanostructures. *Phys. Rev. B* **2007**, *76*, 035438-1–8.
21. Yan, W.; Chen, B.; Mahurin, S. M.; Schwartz, V.; Mullins, D. R.; Lupini, A. R.; Pennycook, S. J.; Dai, S.; Overbury, S. H. J. Preparation and Comparison of Supported Gold Nanocatalysts on Anatase, Brookite, Rutile, and P25 Polymorphs of TiO₂ for Catalytic Oxidation of CO. *J. Phys. Chem. B* **2005**, *109*, 10676–10685.
22. Hutchings, G. J.; Brust, M.; Schmidbaur, H. Gold—An Introductory Perspective. *Chem. Soc. Rev.* **2008**, *37*, 1759–1765.
23. Fierro-Gonzalez, J. C.; Hao, Y.; Gates, B. C. Gold Nanoclusters Entrapped in the α -Cages of Y-Zeolites: Structural Characterization by X-ray Absorption Spectroscopy. *J. Phys. Chem. C* **2007**, *111*, 6645–6651.
24. Guzman, J.; Gates, B. C. Gold Nanoclusters Supported on MgO: Synthesis, Characterization, and Evidence of Au₆. *Nano Lett.* **2001**, *1*, 689–692.
25. Fierro-Gonzalez, J. C.; Gates, B. C. Genesis of Gold Clusters from Mononuclear Gold Complexes on TiO₂: Reduction and Aggregation of Gold Characterized by Time-Resolved X-Ray Absorption Spectroscopy. *J. Phys. Chem. B* **2005**, *109*, 7275–7279.
26. Bus, E.; Prins, R.; van Bokhoven, J. A. Time-Resolved *in Situ* XAS Study of the Preparation of Supported Gold Clusters. *Phys. Chem. Chem. Phys.* **2007**, *9*, 3312–3320.
27. Guzman, J.; Anderson, B. G.; Vinod, C. P.; Ramesh, K.; Niemantsverdriet, J. W.; Gates, B. C. Synthesis and Reactivity of Dimethyl Gold Complexes Supported on MgO: Characterization by Infrared and X-ray Absorption Spectroscopies. *Langmuir* **2005**, *21*, 3675–3683.
28. Uzun, A.; Ortalan, V.; Hao, Y.; Browning, N. D.; Gates, B. C. Imaging Gold Atoms in Site-Isolated MgO-Supported Mononuclear Gold Complexes. *J. Phys. Chem. C* **2009**, *113*, 16847–16849.
29. Wang, S.; Borisavich, A. Y.; Rashkeev, S. N.; Glazoff, M. V.; Sohlberg, K.; Pennycook, S. J.; Pantelides, S. T. Dopants Adsorbed as Single Atoms Prevent Degradation of Catalysts. *Nat. Mater.* **2004**, *3*, 143–146.
30. Mironyuk, I. F.; Gun'ko, V. M.; Povazhnyak, M. O.; Zarko, V. I.; Chelyadin, V. M.; Leboda, R.; Skubiszewska-Zięba, J.; Janusz, W. *Appl. Surf. Sci.* **2006**, *252*, 4071–4082.
31. Okamoto, N. L.; Reed, B. W.; Mehraeen, S.; Kulkarni, A.; Morgan, D. G.; Gates, B. C.; Browning, N. D. Determination of Nanocluster Sizes from Dark-Field Scanning Transmission Electron Microscopy Images. *J. Phys. Chem. C* **2008**, *112*, 1759–1763.
32. Aguilar-Guerrero, V.; Lobo, R. J.; Gates, B. C. Genesis of a Cerium Oxide Supported Gold Catalysts for CO Oxidation: Transformation of Mononuclear Gold Complexes into Clusters as Characterized by X-ray Absorption Spectroscopy. *J. Phys. Chem. C* **2009**, *113*, 3259–3269.
33. Hao, Y.; Gates, B. C. Activation of Dimethyl Gold Complexes on MgO for CO Oxidation: Removal of Methyl Ligands and Formation of Catalytically Active Gold Clusters. *J. Catal.* **2009**, *263*, 83–91.
34. Pyrz, W. D.; Buttrey, D. J. Particle Size Determination Using TEM: A Discussion of Image Acquisition and Analysis for the Novice Microscopist. *Langmuir* **2008**, *24*, 11350–11360.
35. Hackett, S. F. J.; Brydson, R. M.; Gaas, M. H.; Harvey, I.; Newman, A. D.; Wilson, K.; Lee, A. F. High-Activity, Single-Site Mesoporous Pd/Al₂O₃ Catalysts for Selective Aerobic Oxidation of Allylic Alcohol. *Angew. Chem., Int. Ed.* **2007**, *46*, 8593–8596.
36. Akita, T.; Okumura, M.; Tanaka, K.; Kohyama, M.; Haruta, M. Analytical TEM Observation of Au Nanoparticles on Cerium Oxide. *Catal. Today* **2006**, *117*, 62–68.